Elsevier Editorial System(tm) for Construction & Building Materials
Manuscript Draft

Manuscript Number:

Title: Mechanical Behaviors of Steel-Timber Composite Shear Connections

Article Type: Research Paper

Keywords: Steel-timber joints; Shear connector; Self-drilling screw; Push-out tests

Corresponding Author: Miss Ruyuan Yang, Ph.D

Corresponding Author's Institution: Nanjing Forestry University

First Author: Ruyuan Yang, Ph.D

Order of Authors: Ruyuan Yang, Ph.D; Haitao Li; Rodolfo Lorenzo; Youfu Sun; Quan Yuan

Abstract: For extending the structural forms and bearing capacity of timber structures, a novel structural form comprising H-section steel and Larix dahurica glulam was proposed. By conducting static push-out tests on its specimens, their yield and failure modes were observed, and the effects of the shear connector type, diameter, spacing, wood thickness, and other factors on their mechanical properties were analyzed. Finally, the test results were compared to the codes in terms of the bearing capacity, aiming to provide some guidance for practical engineering. According to the results, for specimens of various groups, the yield modes of shear connectors are a uniform "two-hinge" yield, while the failure of joints is characterized by the simultaneous occurrence of the embedding strength failure of glulam flanges and the bending failure of bolts. The ultimate load of joints is directly proportional to the bolt diameter, but it is inversely proportional to the bolt spacing, and it reaches the peak at a wood thickness of 40 mm. The yield load of joints is directly proportional to the bolt diameter, and it reaches the maximum at a wood thickness of 50 mm. Clear differences in the stiffness variation trend between the bolt-connected joints and self-drilling screw (SDS)-connected joints were observed, and the global stiffness of SDS-connected joints is greater than that of bolt-connected joints. The ductility of SDS-connected joints is superior to that of bolt-connected joints, and the joint ductility gradually decreases with the increase in the bolt spacing and reaches its highest level at a wood thickness of 40 mm. For designing the bearing capacity of steel-timber composite joints, the calculation method given in Eurocode 5 is more reasonable.

Suggested Reviewers: Bo Shan
Hunan University
supershanb@hnu.edu.cn

Zheng Li
Department of Structural Engineering, Tongji University
zhengli@tongji.edu.cn

Yang Peng
Nanjing University of Technology
yang.peng@njtech.edu.cn

Cristian Schmitt Rivera
Pontificia Universidad Católica de Chile Santiago
cschmitt@uc.cl

Limin Tian
Xi'an University of Architecture and Technology
tianlimin@xauat.edu.cn

Mechanical Behaviors of Steel-Timber Composite Shear Connections

Ruyuan Yang [a], Haitao Li [b,*], Rodolfo Lorenzo [c], Youfu Sun [a], Quan Yuan [d]

[a] *College of Materials Science and Engineering, Nanjing Forestry University, Nanjing, China.*
[b] *College of Civil Engineering, Nanjing Forestry University, Nanjing, China.*
[c] *University College London, London WC1E 6BT, UK.*
[d] *College of Media and Art, Nanjing University of Information Science & Technology, Nanjing, China.*
[*] *Corresponding Author: Haitao Li. Email: haitao1116@njfu.edu.cn.*

ABSTRACT

For extending the structural forms and bearing capacity of timber structures, a novel structural form comprising H-section steel and *Larix dahurica* glulam was proposed. By conducting static push-out tests on its specimens, their yield and failure modes were observed, and the effects of the shear connector type, diameter, spacing, wood thickness, and other factors on their mechanical properties were analyzed. Finally, the test results were compared to the codes in terms of the bearing capacity, aiming to provide some guidance for practical engineering. According to the results, for specimens of various groups, the yield modes of shear connectors are a uniform “two-hinge” yield, while the failure of joints is characterized by the simultaneous occurrence of the embedding strength failure of glulam flanges and the bending failure of bolts. The ultimate load of joints is directly proportional to the bolt diameter, but it is inversely proportional to the bolt spacing, and it reaches the peak at a wood thickness of 40 mm. The yield load of joints is directly proportional to the bolt diameter, and it reaches the maximum at a wood thickness of 50 mm. Clear differences in the stiffness variation trend between the bolt-connected joints and self-drilling screw (SDS)-connected joints were observed, and the global stiffness of SDS-connected joints is greater than that of bolt-connected joints. The ductility of SDS-connected joints is superior to that of bolt-connected joints, and the joint ductility gradually decreases with the increase in the bolt spacing and reaches its highest level at a wood thickness of 40 mm. For designing the bearing capacity of steel-timber composite joints, the calculation method given in Eurocode 5 is more reasonable.

Keywords: Steel-timber joints, Shear connector, Self-drilling screw, Push-out tests.

1. Introduction

Timber is an ideal building material, and compared to traditional buildings, timber buildings exhibit a series of advantages, including energy conservation, environmental friendliness, high strength-to-weight ratio, renewability, and high cost performance [1-3]. As a material that meets the requirements of environmental friendliness, timber is extensively used for several purposes [4,5]. However, its low design strength and its unsuitability as a tension member have limited the design span and application scope of timber buildings. In this context, the manner to extend structural forms of timber structures and improve their bearing capacity has become an actively researched topic [6-13].

Steel structures are characterized by low self-weight, high bearing capacity, rapid construction progress, and good seismic behavior, but these structures are susceptible to instability. To deal with this issue, a novel section steel-timber composite (STC) member is developed by connecting section steel and timber with shear connectors. In this member, steel serves as the major load-bearing member, while timber renders lateral stiffness for steel, increases the sectional height of the member, and improves its bearing capacity. Compared to conventional steel-concrete composite structures, this STC member can significantly reduce energy consumption, carbon emissions, and self-weight [14,15], It can be used on new-type building structures and bridges. The design of connection joints for members decides the durability and stability of buildings. Shear connectors are mainly used to bear the horizontal shear between the flange and girder and withstand the uplift action between them; hence, they are a key factor that determines whether structures can jointly play their parts [16-18]. Hassanieh et al. [19-21] have used bolts, screws, nail plates, and adhesives, as well as several other methods to connect steel-CLT composite structures and have compared these connection methods in terms of failure modes and load-bearing performance; on this basis, a four-point bending test on STC beams is carried out. Different modes using screws and bolts on STC beams as shear connectors are built, and a nonlinear finite element model for STC beams is established. Loss et al. [22] have connected cold-formed thin-walled section steel and CLT panels with shear connectors and an epoxy resin adhesive and performed a bending performance test. They found that STC structures exhibit an immense development potential in terms of the bearing capacity, stiffness, and construction method. Ataei et al. [23] have investigated the structural performance and energy dissipation capacity of STC joints under cyclic loads and evaluated their ductility, strength loss, and equivalent viscous damping under such conditions. They revealed that STC joints exhibit sound ductility and an energy dissipation capacity. According to a survey of the current literature, STC structures can be promoted as a substitute for traditional steel–concrete composite structures, and effective connection methods available include bolts, screws, nail plates, and adhesives.

For extending the structural forms of timber structures and widening the application scope of domestic Larch, a novel structural form comprising H-section steel and *Larix dahurica* glulam was proposed. By connecting it with different shear connectors and conducting push-out tests on its specimens, their yield and failure modes were observed, and the effects of the shear connector type, diameter, spacing, wood thickness, and other factors on their static mechanical properties were analyzed. Finally, test results were compared to the codes in terms of the bearing capacity, aiming to provide some guidance for practical engineering and making preparations for subsequent tests on composite beams.

2. Experimental tests

2.1. Materials

The used timber specimen is *Larix dahurica* with lumber dimensions of 2000 mm × 150 mm × 40 mm (length × width × height) as the raw material, with a moisture content of 9%-12% after drying. A material test is conducted on the raw material. The basic material properties could be seen in Tab.1. In reference to ANSI A190.1 [24], glulam flanges of two layers (equal in wood thickness) are prepared. Water-proof, weather-resistant phenol-resorcinol-formaldehyde resin adhesive is used, with a single-side spreading rate of 300 g/m^2, a gluing pressure of 1 MPa, a lamination time of 3 h, and a curing time of 6 h. The test begins 7 days after maintenance.

Table 1

Basic properties of *Larix dahurica*.

Air-dried density (g/cm^3)	Parallel-to-grain tensile strength (MPa)	Parallel-to-grain compression strength (MPa)	Parallel-to-grain shear strength (MPa)	Moisture content (%)	Number of specimens
0.67	102.42	50.62	9.50	11.86	20

The used steel specimen is hot-rolled H-section steel, which meets relevant specifications of GB/T50017 [25] and GB/T50011 [26] (model: HW100 × 100; grade: Q235). The dimensions of H-section steel could be seen in Fig.1. For bolt-connected specimens, laser pilot holes are drilled at related positions of the H-section steel flange and timber, and H-section steel and glulam holes are accurately aligned (opening diameter: 1 mm greater than the bolt diameter). For SDS-connected joints, pre-drilling is not necessary, and screws are directly drilled through one side of the timber panel. After penetrating the steel plate, the screws are locked up with the steel plate using a steel thread, thus realizing a tight connection.

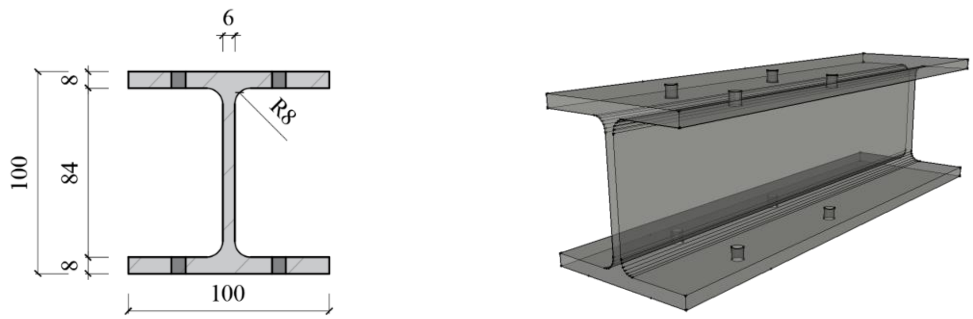

(a) Sectional dimensions (mm) (b) Perspective view

Fig. 1. Dimensional details of H section steel.

Three connectors are used in the test, including two bolts (diameters: 6 mm, 8 mm; length: 80 mm; grade: 6.8), and one SDS (nominal diameter: 5.5 mm; length: 100 mm; material: low-carbon steel). All of these connectors are purchased from Shanghai Meigu C&F Fastener Co., Ltd (Fig.2). The specific test results for the basic material test conducted on connectors could be seen in Tab.2.

(a) SDS bending yield performance test (b) Bolt bending yield performance test (c) Embedding strength performance test

Fig. 2. Test on material properties.

Table 2

Basic properties of connectors.

Connector type	*d* (mm)	Grade	f_{yb} (MPa)	Number	f_{em} (MPa)	Number
Bolt	6	6.8	434.31 (1.26)	12	67.27 (2.55)	15
	8	6.8	451.93 (2.27)	12	61.92 (6.18)	15
SDS	5.5	-	604.98 (2.19)	12	45.19 (7.51)	15

Note: The value in parentheses denotes the variation coefficient (%). In the table, f_{yb} denotes the yield strength of the connector (MPa); and f_{em} denotes the embedding strength of the Larch (MPa).

2.2. Fabrication of specimens

48 specimens are utilized for the test, which are divided into 8 groups. The configuration of specimens could be seen in Fig.3. Specimens of groups A, B, and C exhibit the same connector spacing and wood thickness and use bolts with diameters of 6 mm and 8 mm and SDS with a diameter of 5.5 mm for connection. Specimens of groups D and E comprise the same connector type, diameter, and wood thickness, and the bolt spacing is set to 150 mm and 200 mm, respectively. Specimens of groups F, G, and H comprise the same connector type and spacing, and the glulam flange thicknesses are set to 30 mm,

40 mm, and 60 mm, respectively. All the specimens meet the requirements specified in EN 1995-1-1 [27] for the medium distance, end distance, and edge distance of connectors, as well as the requirements of practical engineering. Connectors are arranged in two columns (each with two connectors), and specimens of each group use connectors of the same type and diameter.

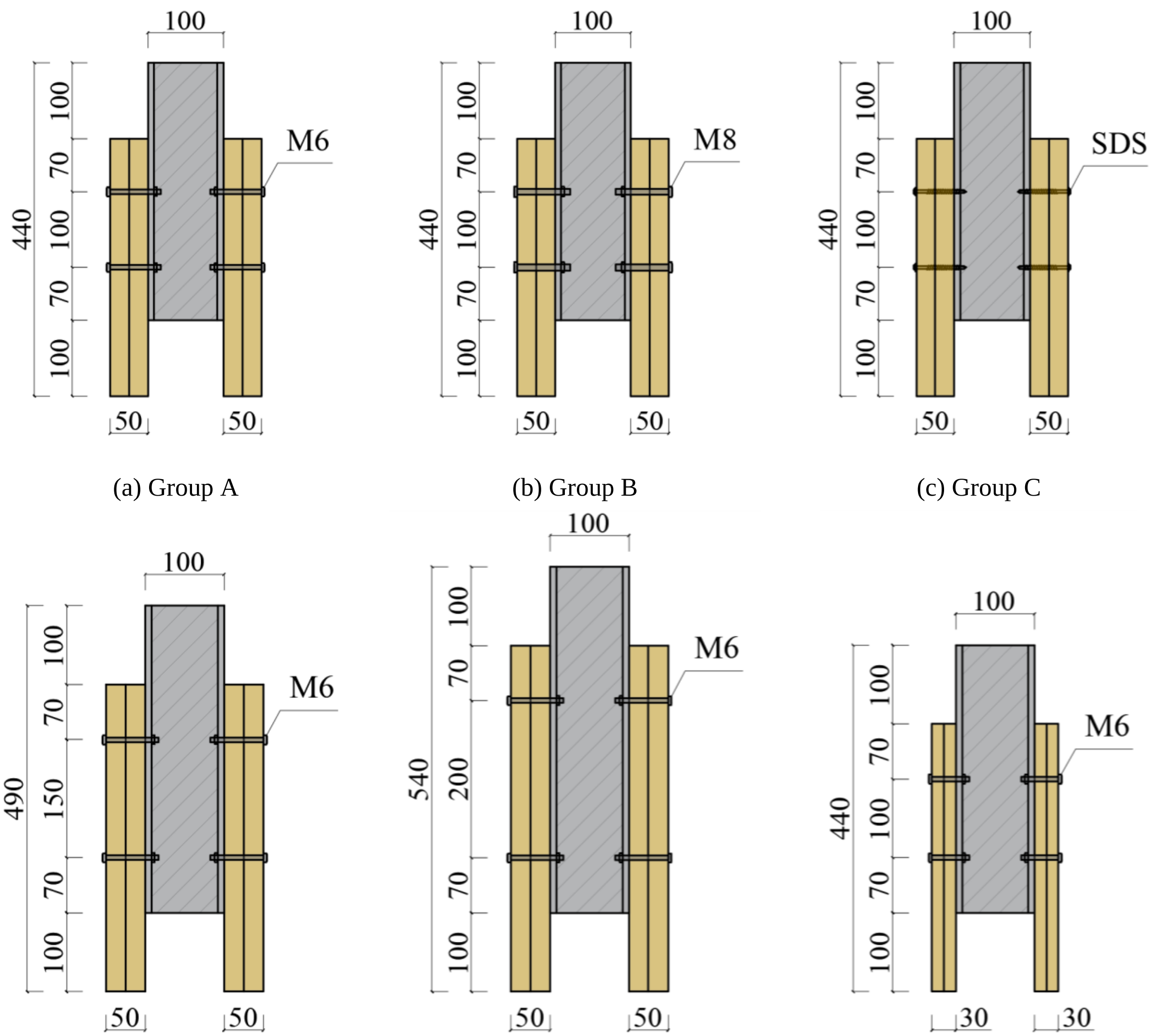

(a) Group A (b) Group B (c) Group C

(d) Group D (e) Group E (f) Group F

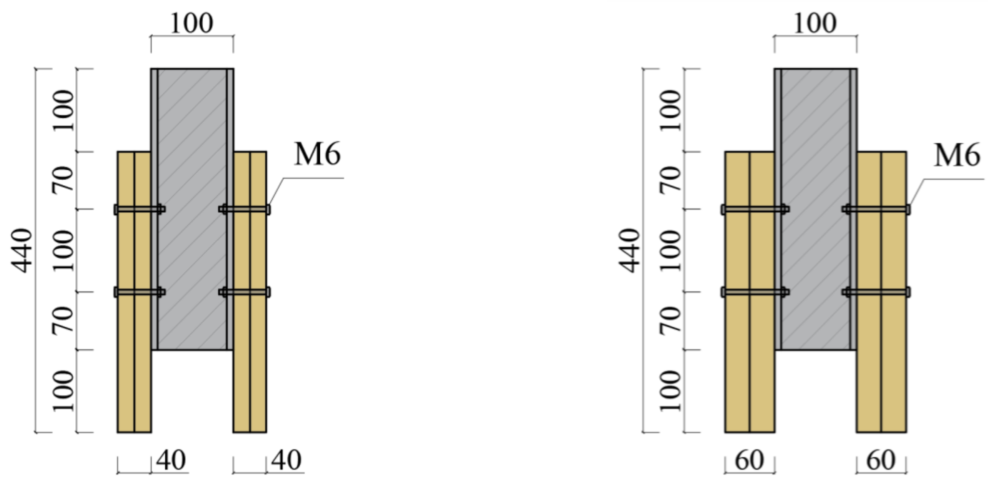

(g) Group G

(h) Group H

Fig. 3. Configuration of specimens (mm).

The specific parameters of specimens of various groups could be seen in Tab.3. Among bolt-connected specimens, those with a bolt diameter of 6 mm use washers with a diameter of 12 mm, and those with a bolt diameter of 8 mm use washers with a diameter of 16 mm.

Table 3

Specific parameters of specimens

Specimen group	t (mm)	Connector type	d (mm)	a_1 (mm)	l (mm)	Number of specimens
Group A	50	Bolt	6	100	340	6
Group B	50	Bolt	8	100	340	6
Group C	50	SDS	5.5	100	340	6
Group D	50	Bolt	6	150	390	6
Group E	50	Bolt	6	200	440	6
Group F	30	Bolt	6	100	340	6
Group G	40	Bolt	6	100	340	6
Group H	60	Bolt	6	100	340	6

Note: In the table, t denotes the glulam flange thickness (mm); d denotes the nominal diameter of the connector (mm); a_1 denotes the parallel-to-grain connector spacing (mm); l denotes the H-section steel and glulam length (mm).

2.3. Arrangement of measurement points and loading regime

Four displacement meters (model: YHD-100) are arranged at the interfaces between H-section steel and glulam to reduce the effects of the initial eccentricity of loads and the uneven distribution of material on the determination of relative slip. The arrangement of displacement meters could be seen in Fig.4. A 10t load sensor (model: M10X) is mounted at the top of H-section steel.

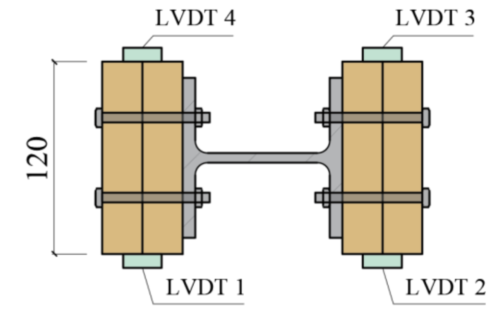

Fig. 4. Arrangement of measuring points (mm).

The main data measured in the test include the applied loads, the relative slip between H-section steel and timber panel, and the strains of steel and timber. The test is performed using a microcomputer-controlled electro-hydraulic servo universal testing machine with a capacity of 100 kN and a TDS-530 data acquisition system. The test scheme could be seen in Fig.5.

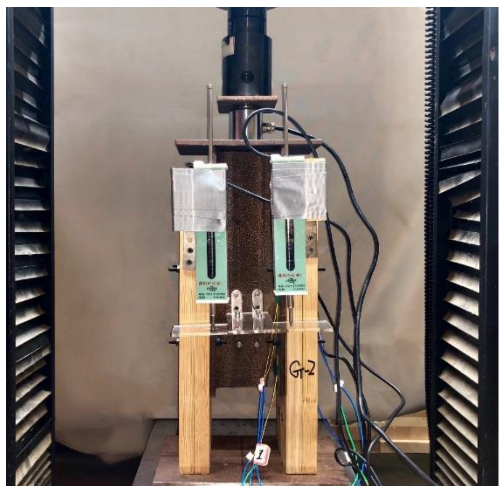

Fig. 5. Test scheme.

The loading regime adopted in the test refers to BS EN 26891 [28]. A typical loading regime could be seen in Fig.6: First, a specimen from each group is selected for monotonic loading at a constant speed (2.41 mm/min) until failure, its maximum load P_{max} is measured, and the maximum value is estimated as the maximum load P_{est}. Next, loads are applied on the other five shear test specimens by grades: (1) loading to 0.4 P_{est} at a constant speed of 0.2 P_{est} /min ± 25% and maintaining it for 30 s; (2) loading to 0.7 P_{est} at a constant speed of 0.2 P_{est} /min ± 25%; (3) after exceeding 0.7 P_{est}, loading at a constant speed to make the specimens fail within 3-5 min. According to BS EN 26891, the specimens exhibit two failure modes: clear fractures in the timber beams on the two sides, and current load is 80% of the peak load P_{max}. Stop loading in either case.

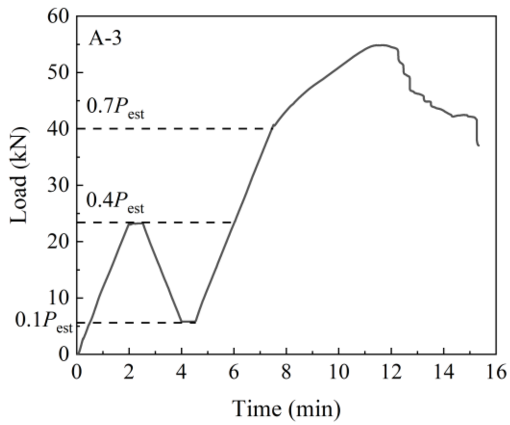

Fig. 6. Typical loading regime (specimen A-3)

3. Test results and discussion

3.1. Failure mode and mechanism

Specimens of various groups exhibited similar failure modes. At the initial stage of loading, the stress of the specimens were relatively stable. Because the specimens were in the elastic stage, the slip showed a linear relationship with the increase of load. With the increase of load, the friction sound between H-section steel and glulam could be heard, and the wood makes a slight sound of being crushed; as a result of the timber being squeezed by nuts or nail heads, glulam subsided locally (Fig.7 (a)), and connectors bended (Fig.7 (b)). Later, the sound of timber being gradually crushed became more intense, and load began to decline after reaching its peak. With the continuation of loading, some connectors failed at the steel-timber joint, and specimens could no longer bear the load. The splitting of the glulam flange on any specimen or clear deformation at any opening of H-section steel was not observed (Fig.7 (c)).

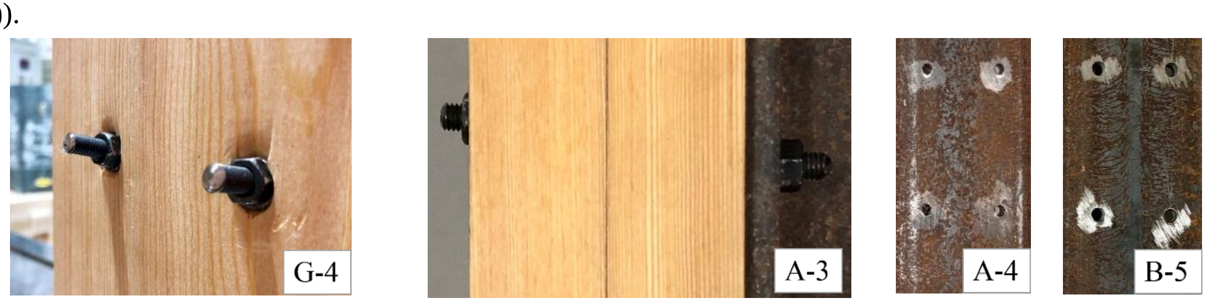

(a) Phenomenon 1 (b) Phenomenon 2 (c) Phenomenon 3

Fig. 7. Experimental phenomena.

Fig.8 shows the failures of typical specimens. Given that there was no clear deformation in H-section steel, crushing of the timber is associated with the formation of two plastic hinges in the dowel connector, with one plastic hinge appearing at the middle and the other in the vicinity of the steel flange, the yield mode could be characterized as “two-hinge” yield (Fig.9.).

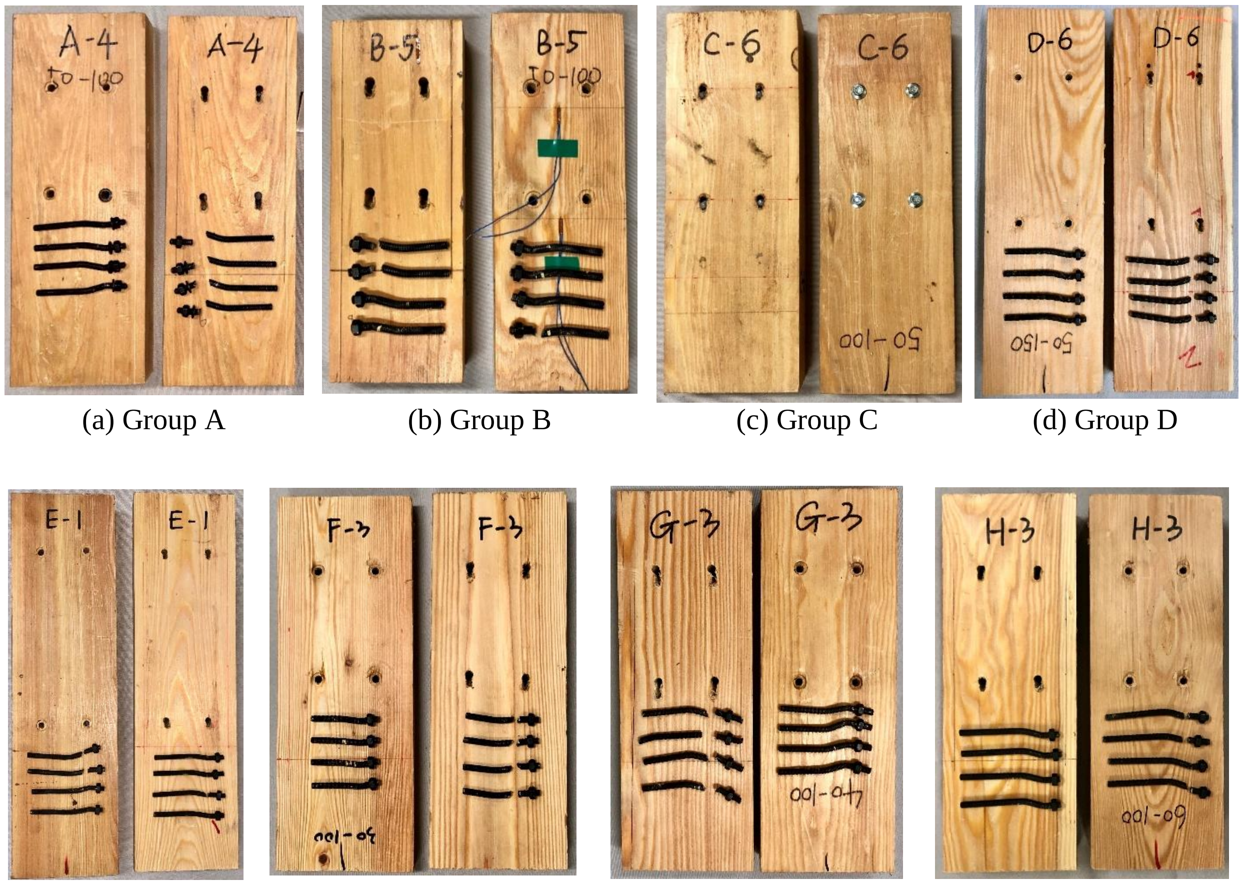

(a) Group A (b) Group B (c) Group C (d) Group D

(e) Group E (f) Group F (g) Group G (h) Group H

Fig. 8. Typical failure modes of specimens of various groups.

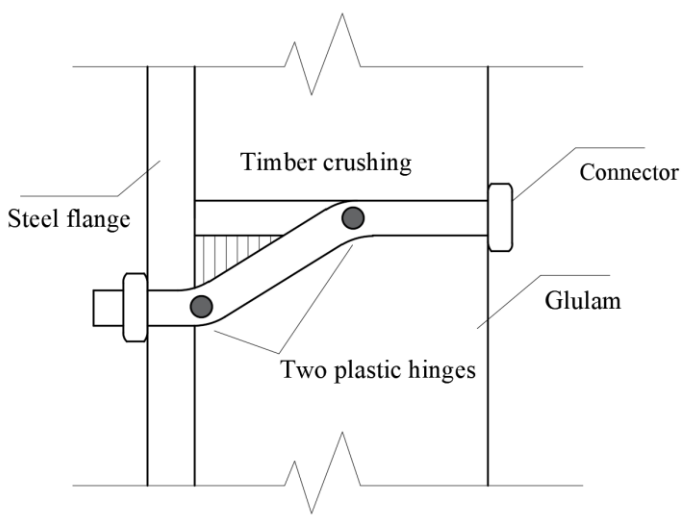

Fig. 9. Characteristics of “two-hinge” yield observed in the steel-timber composite joints.

Splitting of the timber part (Fig.10) revealed the partial embedding failure of the timber close to the joint, the rest of the specimens had no obvious deformation. The joints connected by SDS exhibited relatively ductile behavior, in which the load-slip response revealed a large post-peak branch with a gradual reduction in the strength accompanied by mild softening. However, the joints connected by bolts produced a somewhat brittle mode of failure that was associated with fracture of the bolts.

Fig. 10. Embedding strength failure modes of specimens of various groups.

3.2. Load-slip curve

Fig.11 plots the load-relative slip curves of specimens of various groups:

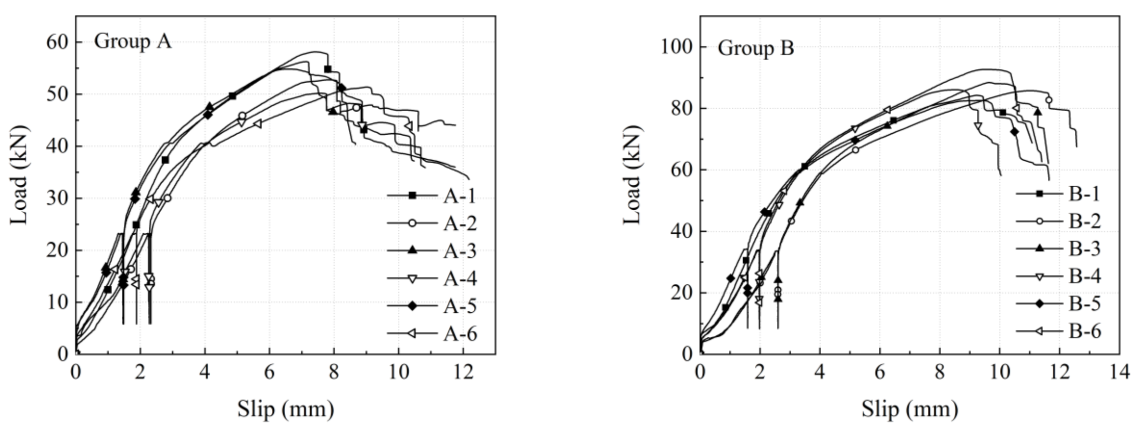

(a) Group A

(b) Group B

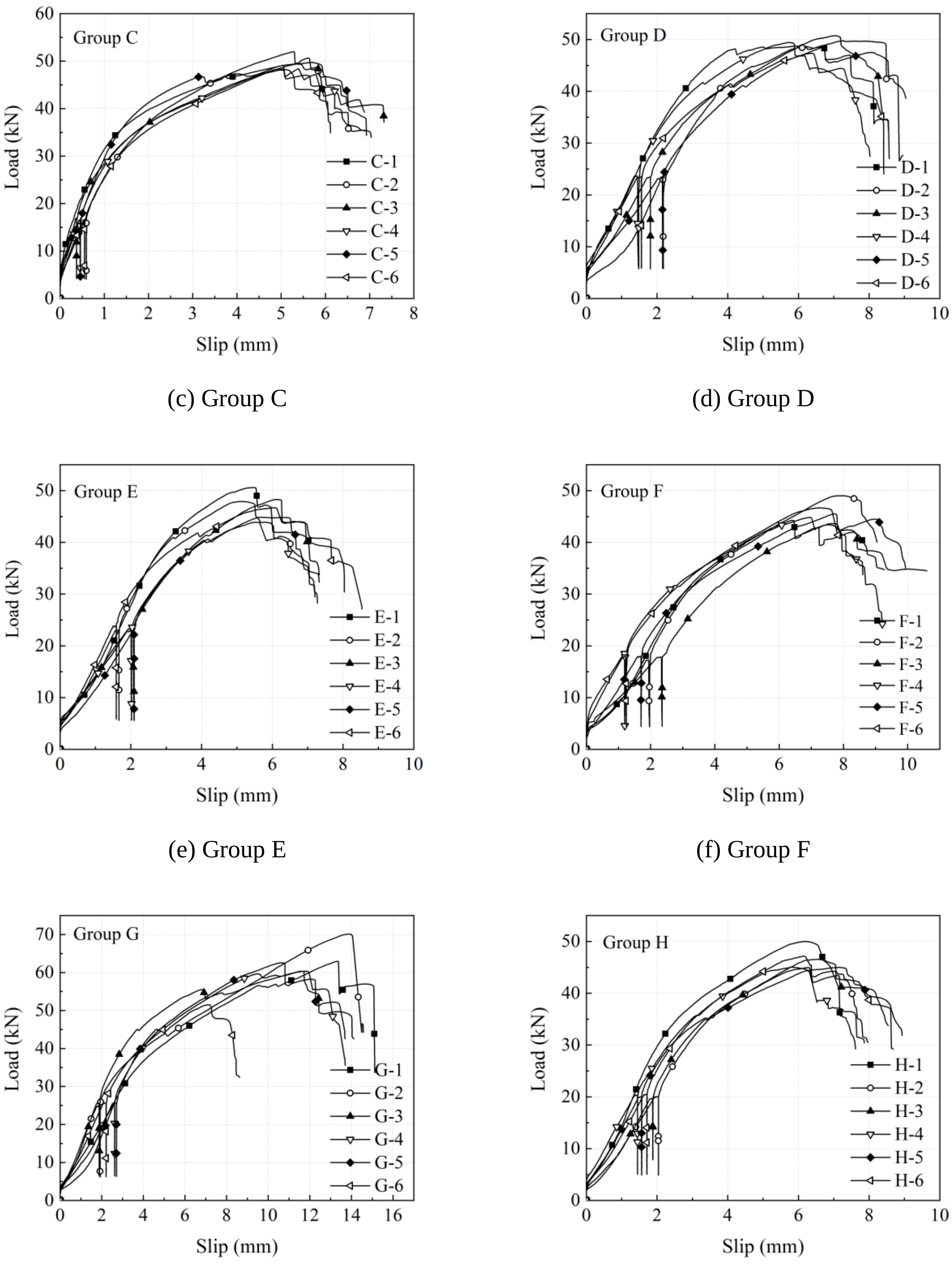

(c) Group C (d) Group D

(e) Group E (f) Group F

(g) Group G (h) Group H

Fig. 11. Load-Slip curves.

The load-relative slip curves of specimens of various groups can be divided into three stages: 1) Elastic stage: At the start of loading, the gradual increase of load causes no clear deformation in the shear connector (corresponding to the no-slip zone in the curve, Fig.12). Taking specimens of group A as an example, when the load reaches ~3.5 kN, the relative slip of the joint begins to grow, and with the continuous increase of the load, it exhibits an approximately linear rising trend. 2) Elastoplastic stage: When the load reaches ~60% of the peak load, slip exhibits nonlinear growth, and it grows at an increasingly rapid pace. 3) Failure stage: After reaching the peak load, the load begins to decline.

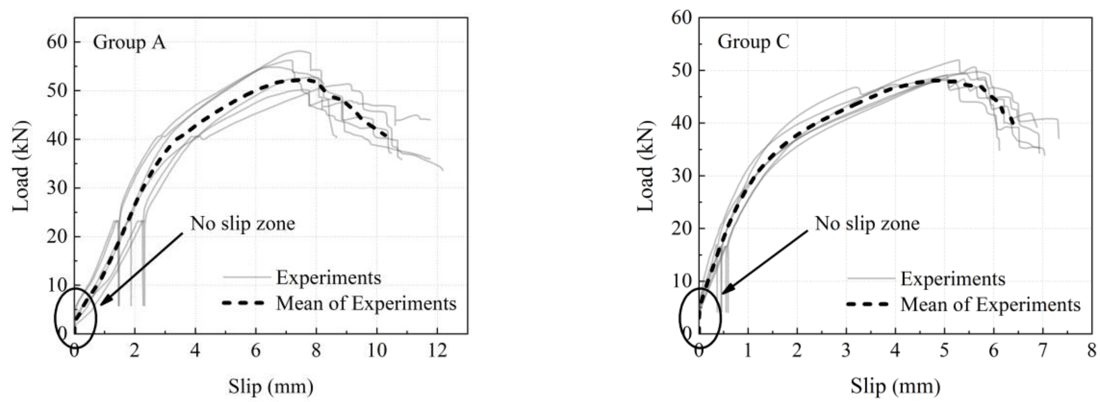

(a) Average curve of specimens of group A (b) Average curve of specimens of group C

Fig. 12. Typical load-slip average curve.

3.3. Analysis of the bearing capacity

Referring to BS EN 12512 [29], 80% of the peak load F_{max} is taken as the ultimate load F_u. Adopting F_u as the horizontal line, the horizontal coordinate of its intersection with the load-slip curve after exceeding the peak load is the ultimate slip V_u. The next step is to draw secant line I based on the two points of 0.1 F_{max} and 0.4 F_{max}, respectively, and tangent line II is drawn relative to the load-slip curve. The dip angle of tangent line II is 1/6 of that of secant line I; the longitudinal and horizontal coordinates of their intersection are yield load F_y and yield slip V_y, respectively. For connection joints, secant stiffness K is an important index for evaluating the connection performance of shear connectors. For reflecting the secant stiffness of shear connectors at different loading stages, the slip stiffness values corresponding to 40%, 60%, and 80% of peak load F_{max} are defined as slip stiffness $K_{0.4}$ in the normal service state, slip stiffness $K_{0.6}$ in the ultimate bearing state, and slip stiffness $K_{0.8}$ in the failure state, respectively. These definitions of secant stiffness have been widely applied to timber composite beams [30,31], which have been calculated according to formula (1). Ductility factor D, defined as the ratio of the ultimate slip V_u to the yield slip V_y, is an index characterizing the working ductility of shear connectors. Fig.13 plots the main data valuation method of BS EN 12512 using specimen B-1 as an example.

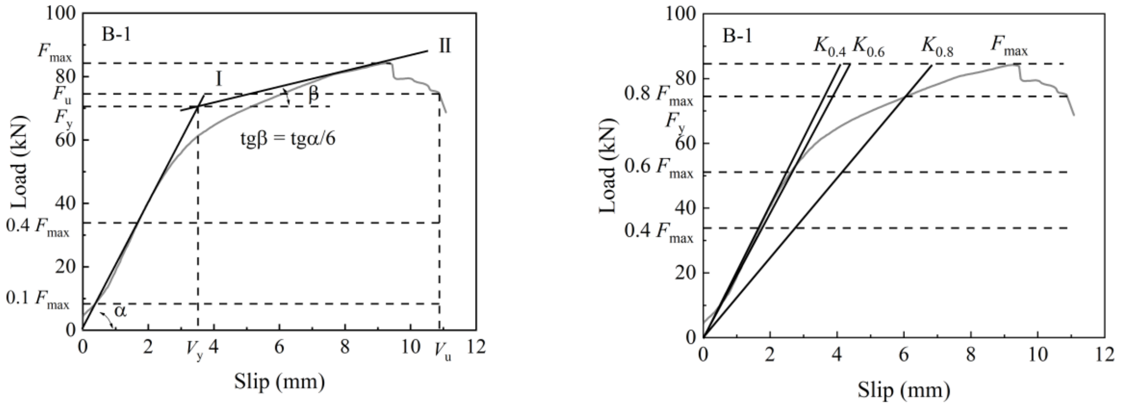

Fig. 13. Main data valuation method of BS EN 12512.

$$K = \frac{F}{v} \tag{1}$$

where K denotes the secant stiffness (kN/mm); F denotes the corresponding load value (kN); and v denotes the relative slip (mm).

The main test results for the specimens of various groups could be seen in Tab.4.:

Table 4

Main test results.

No.	F_{max} (kN)	F_u (kN)	V_u (mm)	F_y (kN)	V_y (mm)	$K_{0.4}$ (kN/mm)	$K_{0.6}$ (kN/mm)	$K_{0.8}$ (kN/mm)	D
Group A	53.92	43.13	9.58	39.65	3.29	12.47	13.43	10.84	2.94
	(5.12)	(5.12)	(9.61)	(4.47)	(14.60)	(15.85)	(15.96)	(12.34)	(9.04)
Group B	86.60	69.28	11.27	61.36	3.75	17.03	17.85	14.15	3.06
	(5.12)	(3.73)	(7.41)	(4.25)	(14.59)	(17.85)	(12.90)	(8.85)	(15.05)
Group C	49.43	39.55	6.53	33.27	1.41	36.51	27.92	17.61	4.73
	(2.58)	(2.58)	(6.98)	(7.96)	(11.67)	(20.41)	(15.19)	(14.98)	(20.18)
Group D	49.09	39.27	8.43	38.52	3.23	12.71	13.67	11.40	2.66
	(2.15)	(2.15)	(5.07)	(7.21)	(14.93)	(17.46)	(15.96)	(11.22)	(13.88)
Group E	47.04	37.63	7.17	39.05	3.38	12.85	13.23	12.02	2.16
	(4.72)	(4.72)	(6.31)	(6.00)	(12.02)	(9.69)	(11.25)	(9.93)	(15.15)
Group F	45.51	36.41	9.21	31.75	3.30	10.74	10.62	8.51	2.88
	(4.30)	(4.30)	(8.75)	(5.07)	(21.92)	(19.42)	(16.19)	(8.77)	(14.31)
Group G	61.30	49.04	13.06	38.63	3.59	11.49	11.50	8.72	3.72
	(8.93)	(8.93)	(16.84)	(7.95)	(14.41)	(13.84)	(11.85)	(10.42)	(23.98)
Group H	46.45	37.16	7.96	34.81	3.08	12.13	12.63	10.49	2.62
	(3.88)	(3.88)	(6.71)	(3.71)	(12.51)	(13.00)	(10.98)	(7.43)	(12.70)

Note: The value in parentheses denotes the variation coefficient (%). In the table, F_{max} denotes the peak load (kN); F_u denotes the ultimate load (kN); V_u denotes the ultimate slip (mm); F_y denotes the yield load (kN); V_y denotes the yield slip (mm); K denotes the secant stiffness (kN/mm); and D denotes the joint ductility factor.

3.3.1. Analysis of the ultimate load and yield load

(1) Ultimate load

The variance analysis results for the ultimate load of joint connections under different factors could be seen in Tab.5. At the level of a = 0.05, significance levels of the effects of the bolt diameter, spacing, and wood thickness on the ultimate load are uniformly 0.00, suggesting that these factors considerably affect the ultimate load.

Table 5

Variance analysis on ultimate load of joint connections under different factors.

Factors	Source	SS	df	MS	F-value	Sig.
Bolt diameter	Inter-group	2,050.95	1	2,050.95	296.11	0.00
	Intra-group	69.26	10	6.93	-	-
	Total	2,120.21	11	-	-	-
Bolt spacing	Inter-group	95.84	2	47.92	13.69	0.00
	Intra-group	52.52	15	3.50	-	-
	Total	148.36	17	-	-	-
Wood thickness	Inter-group	625.60	3	208.53	24.33	0.00
	Intra-group	171.45	20	8.57	-	-
	Total	797.06	23	-	-	-

With the increase in the bolt diameter, the ultimate load of specimens increases on average by 60.79% (Fig.14). As can be known from the above material test, the increase in the bolt diameter leads to the increase in the bending yield strength and embedding strength of individual bolts to varying extents, which is consistent with the results obtained from push-out tests. At a bolt diameter of 6 mm, with the increase in the bolt spacing (Fig.15), the ultimate load of joints gradually decreases, and the magnitude of decrease at a bolt spacing interval of 100–150 mm is greater than that at an interval of 150–200 mm.

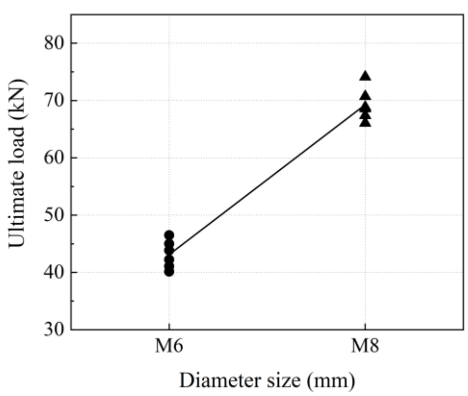

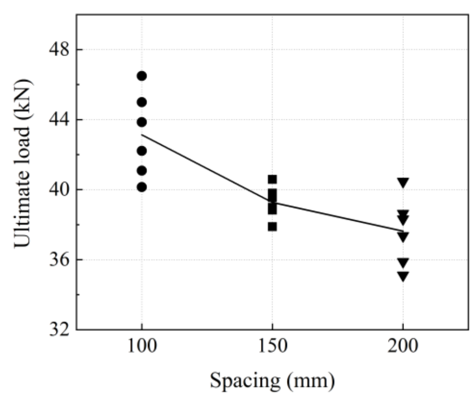

Fig. 14. Relationship between bolt diameter and ultimate load.

Fig. 15. Relationship between bolt spacing and ultimate load.

At a bolt diameter of 6 mm, with the increase in the wood thickness, the ultimate load of joints first increases and then decreases. At a wood thickness of 40 mm, the ultimate load of joints reaches its peak (Fig.16).

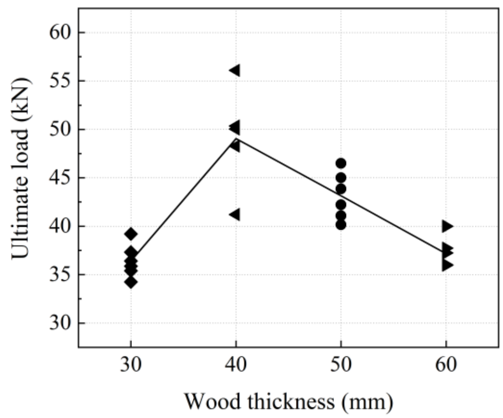

Fig. 16. Relationship between wood thickness and ultimate load.

(2) Yield load

The yield load of joints is an index introduced to measure structural stability, and it exhibits an important function for the bearing stability of joints. The variance analysis on test results could be seen in Tab.6. At the level of a = 0.05, significance levels for the effects of the bolt diameter and wood thickness on the yield load are uniformly 0.00, suggesting that both factors significantly affect the yield load; the significance level for the effect of the bolt spacing on the yield load is 0.75, suggesting that it exhibits a marginal effect on the yield load.

Table 6

Variance analysis on yield load of joint connections under different factors.

Factors	Source	SS	df	MS	F-value	Sig.
Bolt diameter	Inter-group	1,413.76	1	1,413.76	237.09	0.00
	Intra-group	59.63	10	5.96	-	-
	Total	1,473.39	11	-	-	-
Bolt spacing	Inter-group	3.82	2	1.91	0.29	0.75
	Intra-group	98.14	15	6.54	-	-
	Total	101.97	17	-	-	-
Wood thickness	Inter-group	237.04	3	79.01	15.65	0.00
	Intra-group	100.95	20	5.05	-	-
	Total	338.00	23	-	-	-

With the increase in the bolt diameter from 6 mm to 8 mm, the yield load of joints increases on average by 54.57% (Fig.17). With the increase in the glulam flange thickness, the yield load of joints first increases and then decreases; at a wood thickness of 50 mm, the yield load of joints reaches its peak (Fig.18).

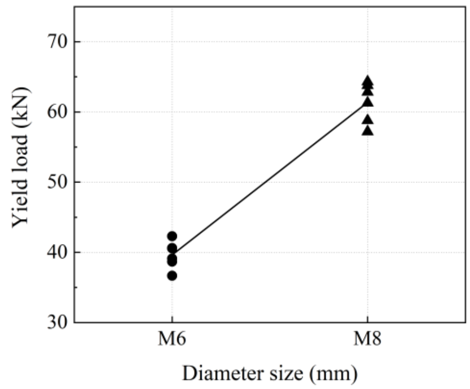

Fig. 17. Relationship between bolt diameter and yield load.

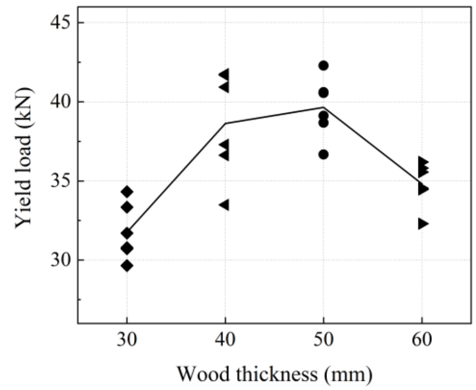

Fig. 18. Relationship between wood thickness and yield load.

3.3.2. Analysis of secant stiffness

The analysis results of the calculated initial stiffness $K_{0.4}$ and secondary stiffness $K_{0.6}$ could be seen in Tab.7. At the level of a = 0.05, the significance level of effects of the bolt diameter on the initial stiffness of the joints $K_{0.4}$ is 0.02, and the significance level of its effect on secondary stiffness $K_{0.6}$ is 0.01, suggesting that the bolt diameter exerts some effect on the secant stiffness and a more significant effect on secondary stiffness. The significance levels of the effect of the bolt spacing on $K_{0.4}$ and $K_{0.6}$ are 0.95 and 0.94, respectively, suggesting that bolt spacing exhibits a slight effect on secant stiffness. The significance levels of the effect of the wood thickness on $K_{0.4}$ and $K_{0.6}$ are 0.47 and 0.07, respectively, suggesting that wood thickness exhibits a slight effect on joint secant stiffness.

Table 7

Variance analysis on secant stiffness *K* of joint connections under different factors.

Secant stiffness	Factors	Source	SS	df	MS	F-value	Sig.
$K_{0.4}$ (kN/mm)	Bolt diameter	Inter-group	62.38	1	62.38	7.91	0.02
		Intra-group	78.86	10	7.89	-	-
		Total	141.24	11	-	-	-
	Bolt spacing	Inter-group	0.46	2	0.23	0.05	0.95
		Intra-group	62.29	15	4.15	-	-
		Total	62.74	17	-	-	-
	Wood thickness	Inter-group	10.46	3	3.49	0.88	0.47
		Intra-group	79.60	20	3.98	-	-
		Total	90.06	23	-	-	-
$K_{0.6}$ (kN/mm)	Bolt diameter	Inter-group	55.74	1	58.74	9.89	0.01
		Intra-group	59.37	10	5.94	-	-
		Total	118.11	11	-	-	-

	Inter-group	0.58	2	0.29	0.06	0.94
Bolt spacing	Intra-group	69.39	15	4.63	-	-
	Total	69.97	17	-	-	-
	Inter-group	27.49	9	9.16	2.69	0.07
Wood thickness	Intra-group	68.01	20	3.40	-	-
	Total	95.50	23	-	-	-

Fig.19 plots the relationship between the connector type and joint secant stiffness. Clear differences in the stiffness variation trend between the bolt-connected joints and SDS-connected joints are observed, and the global stiffness of SDS-connected joints is greater and exhibits rapid degradation. In contrast, the stiffness variation of bolt-connected joints is gentler, and secondary stiffness is slightly greater than the initial stiffness. With the increase in the bolt diameter, the joint secant stiffness exhibits an increasing trend on the whole.

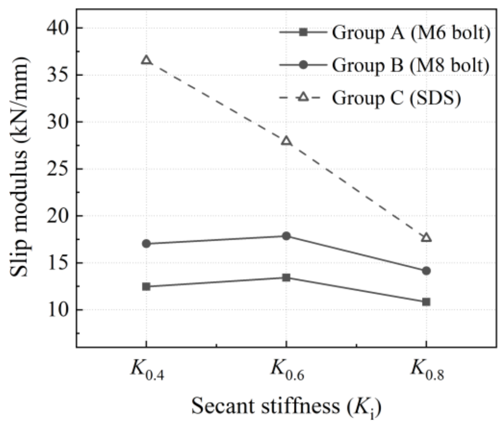

Fig. 19. Relationship between connector type/diameter and secant stiffness.

3.3.3. Analysis of the joint ductility

The analysis results of the calculated joint ductility factor D could be seen in Tab.8. At the level of a = 0.05, the significance level of the effect of the bolt diameter on joint ductility is 0.61, suggesting that bolt diameter slightly affects joint ductility. The significance level of the effect of the bolt spacing on joint ductility is 0.01, suggesting that bolt spacing significantly affects joint ductility. The significance level of the effect of wood thickness on ductility is 0.02, suggesting that wood thickness exhibits some effect on ductility.

Table 8

Variance analysis on ductility of joint connections under different factors.

Factors	Source	SS	df	MS	F-value	Sig.
	Inter-group	0.05	1.00	0.05	0.28	0.61
Bolt diameter	Intra-group	1.70	10.00	0.17	-	-
	Total	1.75	11.00	-	-	-
Bolt spacing	Inter-group	1.88	2.00	0.94	7.50	0.01

	Intra-group	1.88	15.00	0.13	-	-
	Total	3.76	17.00	-	-	-
	Inter-group	4.09	3.00	1.36	3.96	0.02
Wood thickness	Intra-group	6.89	20.00	0.34	-	-
	Total	10.98	23.00	-	-	-

Fig.20 plots the comparison of the joint ductility values among specimens of various groups. In terms of the joints connected by different connectors, the ductility of the joints connected by SDS with a diameter of 5.5 mm is 60.88% greater than that of the joints connected by bolts with a diameter of 6 mm. It is 54.58% greater than that of the joints connected by bolts with a diameter of 8 mm, suggesting that SDS-connected joints exhibit higher ductility. With the increase in the bolt spacing, joint ductility gradually decreases. With the increase in the wood thickness, joint ductility first increases and then decreases, and at a wood thickness of 40 mm, joint ductility reaches its highest value.

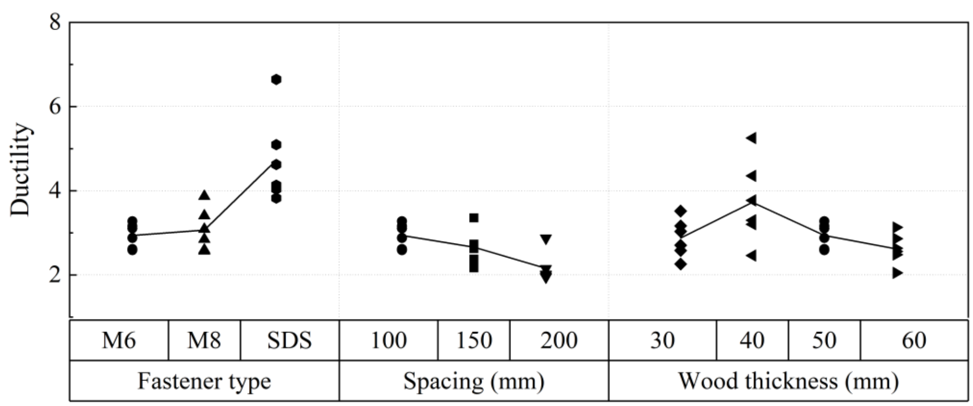

Fig. 20. Comparison of joint ductility among specimens of various groups

3.4. Comparison of test and theoretical values

3.4.1. Calculation of joint bearing capacity according to the Standard for design of timber structures [32]

GB/T 50005-2017 adopts Eurocode-based yield modes, that is, the method of calculating the pin connection bearing capacity proposed by Johansen [33]. It states that, for single-shear or symmetric double-shear pin and shaft fasteners, the design bearing capacity Z_d of each shear plane should be calculated according to formula (2):

$$Z_{\mathrm{d}} = C_{\mathrm{m}} C_{\mathrm{n}} C_{\mathrm{t}} k_{\mathrm{g}} Z \quad (2)$$

where C_m denotes the adjustment coefficient of moisture content, set as $C_m = 1.00$ (in the test, the moisture content of glulam members is less than 15%); C_n denotes the adjustment coefficient of design service life, which is set at $C_n = 1.00$ (according to the *Code for design of the municipal bridges* [34], and the design service life for small- and medium-span timber bridges is 50 years); C_t denotes the adjustment coefficient of temperature, set as 1.00; k_g denotes the combination coefficient of bolts, set as 1.00; and Z denotes the reference design bearing capacity, which can be calculated according to formula (3):

$$Z = k_{\min} t_{\mathrm{s}} d f_{\mathrm{es}} \quad (3)$$

where t_s denotes the H-section steel flange thickness (mm); d denotes the connector diameter (mm); f_{es} denotes the connector embedding strength on steel, set as 445.50 MPa (calculated by 1.1 times of the design embedding strength of grade Q235 section steel; k_{min} denotes the minimum effective length factor of the embedding strength of section steel (the failure mode in the test is yield mode IV (Fig.21)), which can be determined according to formula (4):

$$k_{\mathrm{IV}} = \frac{d}{1.88t_{\mathrm{s}}}\sqrt{\frac{1.647R_{\mathrm{e}}k_{\mathrm{ep}}f_{\mathrm{yb}}}{3\left(1+R_{\mathrm{e}}\right)f_{\mathrm{es}}}} \tag{4}$$

$$R_{\mathrm{e}} = \frac{f_{\mathrm{em}}}{f_{\mathrm{es}}} \tag{5}$$

where k_{ep} denotes elastoplasticity strengthening coefficient, set as 1.00; f_{yb} denotes the bolt bending yield strength (MPa); and f_{em} denotes the embedding strength of the timber (MPa).

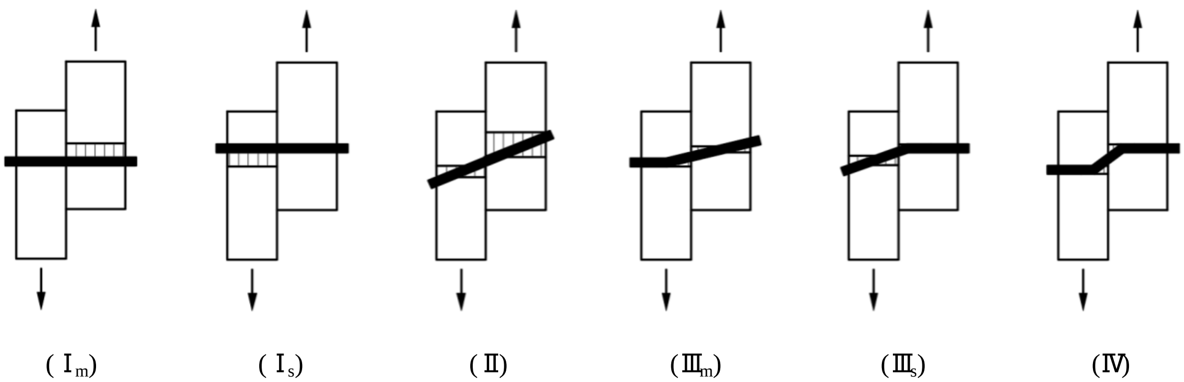

Fig. 21. Several failure modes of simple shear connections in GB/T 50005-2017 and NDS-2018

3.4.2. Calculation of the bearing capacity of connectors in NDS

According to the *National Design Specification for Wood Construction* [35], the design bearing capacity Z_d of each shear plane of simple shear connections is expressed as follows:

$$Z_{\mathrm{d}} = nC_{\mathrm{g}}Z \tag{6}$$

$$Z = \frac{d^2}{R_{\mathrm{d}}}\sqrt{\frac{2f_{\mathrm{em}}f_{\mathrm{yb}}}{3\left(1+R_{\mathrm{e}}\right)}} \tag{7}$$

$$C_{\mathrm{g}} = \begin{cases} 1.0 & \text{(a)} \\ \left|\dfrac{m\left(1-m^{2\mathrm{n}}\right)}{n\left[\left(1+R_{\mathrm{EA}}m^{\mathrm{n}}\right)\left(1+m\right)-1+m^{2\mathrm{n}}\right]}\right| & \text{(b)} \end{cases} \tag{8}$$

$$m = u-\sqrt{u^2-1} \tag{9}$$

$$u = 1+\gamma\frac{a_1}{2}\left(\frac{1}{E_{\mathrm{m}}A_{\mathrm{m}}}+\frac{1}{E_{\mathrm{s}}A_{\mathrm{s}}}\right) \tag{10}$$

$$R_{\mathrm{EA}} = \frac{E_{\mathrm{m}}A_{\mathrm{m}}}{E_{\mathrm{s}}A_{\mathrm{s}}} \tag{11}$$

where n denotes the parallel-to-grain number of connectors in each column; Z denotes the bearing capacity of each shear plane of each fastener (N); C_g denotes cohort effect influence factor, set as 1.00 when the connector diameter is less than 6.35 mm and calculated according to formula (8 (b)) when the connector diameter is no less than 6.35 mm; R_d denotes the reduction factor, set as $R_d = 3.2$ when 6.35 mm $\leq d \leq$ 25.4 mm, and as $R_d = 0.39d + 0.5$ when $d <$ 6.35 mm; γ denotes the joint shear slip modulus (kN/mm), set as 270,000 $(d/25.4)^{1.5}$ in the case of steel–timber connections; a_1 denotes the parallel-to-grain bolt spacing (mm); E_m denotes the elasticity modulus of the timber (GPa); E_s denotes the elasticity modulus of section steel (GPa); A_m denotes the sectional area of the timber (mm^2); and A_s denotes the sectional area of section steel (mm^2).

3.4.3 Calculation of the bearing capacity of bolts in Eurocode 5

In Eurocode 5, the bearing capacity Z_d of multi-bolt-connected joints is calculated according to the following formula:

$$Z_{\mathrm{d}} = n_{\mathrm{ef}} Z \tag{12}$$

$$n_{\mathrm{ef}} = \begin{cases} n_{\mathrm{t}} n^{k_{\mathrm{ef}}} & \text{(a)} \\ n_{\mathrm{t}} n^{0.9} \sqrt[4]{\dfrac{a_1}{13d}} & \text{(b)} \end{cases} \tag{13}$$

where n_{ef} denotes the parallel-to-grain valid number of bolts in a column, calculated according to formula (13 (a)) in the case of specimens using nailed joints (given that, for specimens of group C, $a_1 \geq 14d$ and $k^{ef} = 1$, it is calculated according to formula (13 (b)) for bolt-connected specimens); and n_t denotes the number of bolt columns.

According to the classification of the specimen failure modes given in EN1995-1-1 (Fig.22), the test falls within the scope of the yield mode. In this mode, the bearing capacity of the shear plane of each fastener is calculated according to formula (14):

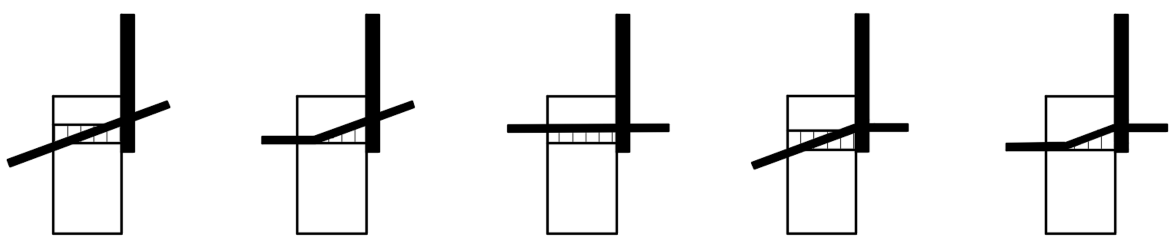

(a) (b) (c) (d) (e)

Fig. 22. Several failure modes of simple shear connections in Eurocode 5

$$Z = 2.3\sqrt{M_{\mathrm{y,Rk}} f_{\mathrm{em}} d} + \frac{F_{\mathrm{ax,Rk}}}{4} \tag{14}$$

where $M_{y,Rk}$ denotes the yield moment of the fastener (N·mm); and $F_{ax, Rk}$ denotes the nail-holding power of the fastener (N).

3.4.4. Comparison of test and theoretical values

The results obtained for the joint bearing capacity calculated according to codes of various countries could be seen in Tab.9. From this table, the values calculated according to GB/T 50005-2017 and

NDS-2018 are similar, with error ranges of 43.04%–54.83% and 58.74%–66.96%, respectively. As can be seen from Fig.23, the values calculated according to Eurocode 5 are similar to the joint yield strength values obtained from the test, suggesting that the calculation method given in Eurocode 5 is more reasonable for designing the bearing capacity of STC joints.

Table 9

Calculated results of theoretical values in codes of various countries.

Group No.	F_y (kN)	GB/T 50005-2017 (kN)	NDS-2018 (kN)	Eurocode 5 (kN)
Group A	39.65	18.08 (54.39)	13.10 (66.96)	43.31 (9.22)
Group B	61.36	31.63 (48.45)	20.48 (66.63)	70.34 (14.63)
Group C	33.27	15.03 (54.83)	11.66 (64.96)	36.39 (9.38)
Group D	38.52	18.08 (53.05)	13.10 (65.99)	47.93 (24.42)
Group E	39.05	18.08 (53.69)	13.10 (66.45)	51.50 (31.88)
Group F	31.75	18.08 (43.04)	13.10 (58.74)	43.31 (36.40)
Group G	38.63	18.08 (53.19)	13.10 (66.09)	43.31 (12.10)
Group H	34.81	18.08 (48.05)	13.10 (62.37)	43.31 (24.41)

Note: The value in parentheses denotes error (%), error = [(code calculated value − test value)/test value] × 100%.

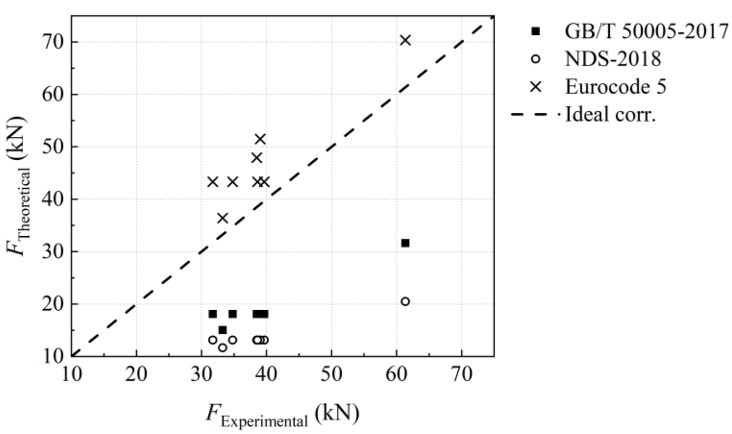

Fig. 23. Comparison between the values obtained from the experimental tests and the corresponding theoretical values given by GB/T 50005-2017, NDS-2018, and Eurocode 5.

4. Summary and conclusion

Considering that connection joints constitute the key to designing STC structures, static push-out tests on STC-connected joints are carried out, and differences in the bearing capacity, stiffness, ductility, and other performance parameters by using different connector types, diameters, spacing, and glulam flange thicknesses are compared. Based on test results and analysis, the following conclusions can be drawn:

(1) For specimens of various groups, the yield modes of shear connectors are uniformly “two-hinge” yield, while the failure of joints is characterized by the simultaneous occurrence of the embedding strength failure of glulam flanges and the bending failure of bolts.

(2) The bolt diameter, spacing, and wood thickness significantly affect the ultimate load of joints: The ultimate load of joints is directly proportional to the bolt diameter, but it is inversely proportional to the bolt spacing, and it reaches the peak at a wood thickness of 40 mm. The bolt diameter and wood thickness significantly affect the yield load of joints: The yield load of joints is directly proportional to the bolt diameter, and reaches its maximum at a wood thickness of 50 mm. The bolt spacing slightly affects the yield load.

(3) Clear differences in the stiffness variation trend between bolt-connected joints and SDS-connected joints are observed, and the global stiffness of SDS-connected joints is greater and exhibits rapid degradation. In contrast, the stiffness variation of bolt-connected joints is gentler, and the secondary stiffness is slightly greater than the initial stiffness. With the increase in the bolt diameter, joint secant stiffness exhibits an increasing trend on the whole.

(4) The ductility of SDS-connected joints is superior to that of bolt-connected joints. The bolt diameter slightly affects the joint ductility, and the bolt spacing significantly affects the joint ductility. With the increase in the bolt spacing, the joint ductility gradually decreases, and at a wood thickness of 40 mm, the joint ductility reaches its highest level.

(5) By comparing test results with the results calculated according to GB/T 50005-2017, NDS-2018, and Eurocode 5, the results calculated according to Eurocode 5 are similar to the test results, and errors are observed in the case of GB/T 50005-2017 and NDS-2018. Thus, for designing the bearing capacity of STC joints, the calculation method given in Eurocode 5 is more reasonable.

Declaration of Competing Interest

The authors declare that they have no known competing financial interests or personal relationships that could have appeared to influence the work reported in this paper.

Acknowledgements

This research is supported by the Natural Science Foundation of Jiang-su Province (Grant No. BK20181402), the National Natural Science Foundation of China (Grant No. 51878354), a Project Funded by the National First-class Disciplines (PNFD), a Project Funded by the Priority Academic Program Development of Jiangsu Higher Education Institutions (PAPD), and a Project Funded by Nanjing Forestry University Co-Innovation Center of Efficient Processing and Utilization of Forest Resources. Any research results expressed in this paper are those of the writer(s) and do not necessarily reflect the views of the foundations.

References

[1] M. He, F. Lam, J. Yang, S. Zhang, Wood Structural Design. China Construction Industry Press, 2008.
[2] Y. Sun, X. Yang, On the development prospect of Chinese wood structural architecture, Building Materials Decoration. 6 (2011) 22-26.
[3] Z. Yuan, Y. Sun, Thermal insulation materials for wood structures, Decoration of Building Materials. 6 (2015) 23-25.
[4] X. Li, M. Ashraf, H. Li, X. Zheng, H. Wang, S. Al-Deen, P. J. Hazell, An experimental investigation on parallel bamboo strand lumber specimens under quasi static and impact loading, Construction and Building Materials. 228 (2019) 116724.
[5] D. Bigot, C. Ott, S. Guichard, B. Malet-Damour, Feasibility of using wood chips to regulate relative humidity inside a building: a numerical study, Journal of Renewable Materials. 7(6) (2019) 505-516.
[6] D. Denouwe, M. Adamah, F. Eric, B. Abdelhamid, Experimental study of the mechanical behavior of timber-concrete shear connections with threaded reinforcing bars, Engineering Structures. 172 (2018)

997-1010.

[7] H. Yang, W. Liu, J. Shao, Z. Zhou, Bending behavior of FRP reinforced wood beams, Journal of Building Materials. 05 (2008) 591-597.

[8] H. Li, G. Wu, Q. Zhang, A. Deeks, J. Su, Ultimate bending capacity evaluation of laminated bamboo lumber beams, Construction and Building Materials. 160 (2017) 365-375.

[9] H. Zhang, H. Li, I. Corbi, O. Corbi, G. Wu, C. Zhao,T. Cao, AFRP influence on parallel bamboo strand lumber beams, Sensors. 18(9) (2018) 2854.

[10] P. Shang, Y. Sun, D. Zhou, K. Qin, X. Yang, Experimental study of the bending performance of hollow glulam beams, Wood and Fiber Science. 50(1) (2018) 3-19.

[11] H. Li, Z. Qiu, G. Wu, O. Corbi, L. Wang, I. Corbi, C. Yuan, Slenderness ratio effect on eccentric compression performance of parallel strand bamboo lumber columns, Journal of Structural Engineering ASCE. 145(8) (2019) 04019077.

[12] H. Li, R. Liu, R. Lorenzo, G. Wu, L. Wang, Eccentric compression properties of laminated bamboo lumber columns with different slenderness ratios. Proceedings of the Institution of Civil Engineers - Structures and Buildings. 172(5) (2019) 315-326.

[13] C. Tan, H. Li, D. Wei, R. Lorenzo, C. Yuan, Mechanical performance of parallel bamboo strand lumber columns under axial compression: experimental and numerical investigation, Construction and Building Materials. 231 (2020) 117168.

[14] F. Nouri, H. Valipour, Semi-rigid partial-strength steel-timber composite (STC) connections with mechanically anchored steel rods, Journal of Constructional Steel Research. 158 (2019) 560-575.

[15] L. Aye, T. Ngo, R. Crawford, R. Gammampila, P. Mendis, Life cycle greenhouse gas emissions and energy analysis of prefabricated reusable building modules, Energy Build. 47 (2012) 159-168.

[16] C. Fang, Analysis of static performance in steel-wood connection (MA. Thesis), Beijing Jiaotong University, 2015.

[17] G. Wu, Y. Zhong, Y. Gong, H. Ren, Application of modern wood product glulam in timber frame with tenon-mortise joints and its structural behavior. Journal of Renewable Materials, 7(5) (2019) 451-461.

[18] Z. Shu, Z. Li, X. Yu, J. Zhang, M. He, Rotational performance of glulam dowel type bolted joints: experimental investigation and analytical approach, Construction and Building Materials. 213 (2019) 675-695.

[19] A. Hassanieh, H. Valipour, M. Bradford, Load-slip behaviour of steel-cross laminated timber (CLT) composite connections, Journal of Constructional Steel Research. 122 (2016) 110-121.

[20] A. Hassanieh, H. Valipour, M. Bradford, Experimental and numerical study of steel-timber composite (stc) beams, Journal of Constructional Steel Research. 122 (2016) 367-378.

[21] A. Hassanieh, H. Valipour, M. Bradford, Experimental and analytical behaviour of steel-timber composite connections, Construction and Building Materials. 118 (2016) 63-75.

[22] C. Loss, B. Davison, Innovative composite steel-timber floors with prefabricated modular components, Engineering Structures. 132 (2017) 695-713.

[23] A. Ataei, A. Chiniforush, M. Bradford, H. Valipour, Cyclic behaviour of bolt and screw shear connectors in steel-timber composite (STC) beams, Journal of Constructional Steel Research. 161 (2019) 328-340.

[24] ANSI A190.1-2012 Standard for wood products-Structural glued laminated timber. American Society for Testing and Materials, 2012.

[25] GB/T 50017 Code for design of steel structure. China Building Industry Press, 2017.

[26] GB/T 50011 Code for seisnuc design of buildings. China Building Industry Press, 2010.

[27] EN 1995-1-1 Eurocode 5: Design of timber structures - Part 1-1: General - Common rules and rules for buildings. European committee for standardization, 2004.

[28] BS EN 26891-1991 Timber structures - Joints made with mechanical fasteners - General principles for the determination of strength and deformation characteristics. British Standards Institution, 2000.

[29] BS EN 12512-2001 Timber structures - Test methods - Cyclic testing of joints made with mechanical fasteners. British Standards Institution, 2001.

[30] D. Yeah, M. Fragiacomo, B. Deam, Experimental behavior of LVL-concrete composite floor beam at strength limit state. Engineering Structures. 45(12) (2014) 4384-4392.

[31] Y. Wei, C. Yang, Z. Wang, L. Zhao, M. Duan, Mechanical properties of notch-dowel connections of bamboo-concrete, Journal of Forestry Engineering, 3(6) (2018) 135-141.

[32] GB/T 50005 Code for design of timber structures. China Building Industry Press, 2017.

[33] K. Johansen, Theory of timber connections, International Association of Bridge and Structural Engineering. 9 (1949) 249-262.
[34] CJJ11 Code foe design of the municipal bridge. China Building Industry Press, 2011.
[35] NDS-2017 National Design Specification for Wood Construction. American Wood Council, 2017.

HIGHLICHTS

- Considering various shear connector type, diameter, spacing and wood thickness, a novel structural form comprising H-section steel and *Larix dahurica* glulam was proposed.
- The ultimate load of joints is directly proportional to the bolt diameter, but it is inversely proportional to the bolt spacing. The yield load of joints is directly proportional to the bolt diameter.
- Clear differences in the stiffness variation trend between the bolt-connected joints and self-drilling screw (SDS)-connected joints were observed, and the global stiffness of SDS-connected joints is greater than that of bolt-connected joints.
- The ductility of SDS-connected joints is superior to that of bolt-connected joints, and the joint ductility gradually decreases with the increase in the bolt spacing.
- For designing the bearing capacity of steel-timber composite joints, the calculation method given in Eurocode 5 is more reasonable.

***Declaration of Interest Statement**

Declaration of interests

☒ The authors declare that they have no known competing financial interests or personal relationships that could have appeared to influence the work reported in this paper.

☐The authors declare the following financial interests/personal relationships which may be considered as potential competing interests: